Supercooling of Atoms in an Optical Resonator

Minghui Xu,[1,2] Simon B. Jäger,[3] S. Schütz,[3] J. Cooper,[1] Giovanna Morigi,[3] and M. J. Holland[1,2]

[1]*JILA, National Institute of Standards and Technology and Department of Physics,*
University of Colorado, Boulder, Colorado 80309-0440, USA
[2]*Center for Theory of Quantum Matter, University of Colorado, Boulder, Colorado 80309, USA*
[3]*Theoretische Physik, Universität des Saarlandes, D-66123 Saarbrücken, Germany*

We investigate laser cooling of an ensemble of atoms in an optical cavity. We demonstrate that when atomic dipoles are synchronized in the regime of steady-state superradiance, the motion of the atoms may be subject to a giant frictional force leading to potentially very low temperatures. The ultimate temperature limits are determined by a modified atomic linewidth, which can be orders of magnitude smaller than the cavity linewidth. The cooling rate is enhanced by the superradiant emission into the cavity mode allowing reasonable cooling rates even for dipolar transitions with ultranarrow linewidth.

The discovery of laser cooling [1] has enabled new areas of quantum gas physics and quantum state engineering [2]. Laser cooling is an essential technology in many fields, including precision measurements, quantum optics, and quantum information processing [3–5]. Doppler laser cooling [6,7] relies on repeated cycles of electronic excitation by lasers followed by spontaneous relaxation, reaching temperature limits determined by the atomic linewidth. Only specific atomic species can be Doppler cooled because they should possess an internal level structure that allows for closed cycling transitions.

Cavity-assisted laser cooling [8,9] utilizes the decay of an optical resonator instead of atomic spontaneous emission for energy dissipation. It is based on the preferential coherent scattering of laser photons into an optical cavity [10,11]. Temperatures that can be achieved in this way are limited by the cavity linewidth. Since the particle properties enter only through the coherent scattering amplitude, cavity-assisted cooling promises to be applicable to any polarizable object [12–20], including molecules [17,18] and even mesoscopic systems such as nanoparticles [19,20].

The many-atom effects of cavity-assisted cooling were theoretically discussed by Ritsch and collaborators [21] and experimentally reported [22,23]. The cavity-mediated atom-atom coupling typically leads to a cooling rate that is faster for an atomic ensemble than for a single atom. Self-organization may occur and is observed as patterns in the atomic distribution that maximize the cooperative scattering. Recently, it has been shown that the long-range nature of the cavity-mediated interaction between atoms gives rise to interesting prethermalization behavior [24]. In spite of the intrinsic many-body nature, the underlying cooling mechanism shares much with the single-atom case, and indeed the final temperature observed in these systems is limited by the cavity linewidth.

In this Letter, we demonstrate that the mechanical action of the atom-cavity coupling takes on a dramatically new character for atoms in the regime of steady-state super-radiance [25–30]. Specifically, the frictional force on a single atom is significantly enhanced, and the final temperature is much lower than the temperature that can be achieved in cavity-assisted cooling [10,11]. Furthermore, as the atom number increases, the cooling may become faster due to the increasing rate of superradiant collective emission. We show that ability to achieve much lower temperatures than for single-atom cavity-assisted cooling derives from the emergence of atom-atom dipole correlations in the many-body atomic ensemble.

Steady-state superradiant lasers were proposed in Ref. [25] as possible systems for generating milliHertz linewidth light, and demonstrated in a recent experiment using a two-photon Raman transition [27]. In steady-state superradiance, the cavity decay is much faster than all other processes and plays the role of a dissipative collective coupling for the atoms that leads to the synchronization of atomic dipoles [29,30]. The emergence of a macroscopic collective dipole induces an extremely narrow linewidth for the generated light [25,30]. The optimal parameters are in the weak-coupling regime of cavity QED [31], which is opposite to the strong-coupling situation usually considered in cavity-assisted cooling [8,9]. Superradiant lasers require weak-dipole atoms (e.g., using intercombination lines or other forbidden transitions) confined in a high-finesse optical cavity.

We consider an ensemble of N pointlike two-level atoms with transition frequency ω_a and natural linewidth γ, interacting with a single-mode cavity with resonance frequency ω_c and linewidth κ, as shown in Fig. 1. The atoms are restricted to move freely along the direction of the cavity axis (x axis) and are tightly confined in the other two directions. The atom-cavity coupling is given by $g\cos(kx)$, where g is the vacuum Rabi frequency at the
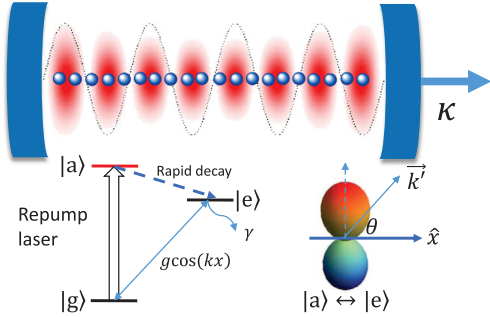
FIG. 1. Atoms with ultranarrow transition $|g\rangle \leftrightarrow |e\rangle$ are confined to the axis of a standing-wave mode of an optical cavity. Different implementations of pumping may be considered [25,27]. In the simplest scenario shown, a transition is driven from the ground state $|g\rangle$ to an auxiliary state $|a\rangle$ that rapidly decays to the excited state $|e\rangle$. In this way $|a\rangle$ can be adiabatically eliminated and a two-state pseudospin description in the $\{|g\rangle, |e\rangle\}$ subspace used, with repumping corresponding to an effective rate w from $|g\rangle$ to $|e\rangle$. If the repumping laser is directed normal to the cavity axis, the absorption does not modify the momentum. Momentum recoil is induced by the on-axis component of the wave vector $\vec{k}'$ of the dipole radiation pattern for the $|a\rangle \leftrightarrow |e\rangle$ transition.

field maximum, and $\cos(kx)$ describes the one-dimensional cavity mode function [32]. The atoms are incoherently repumped at rate w, providing the photon source.

The Hamiltonian in the rotating frame of the atomic transition frequency is given by

$$\hat{H} = \hbar\Delta\hat{a}^\dagger\hat{a} + \sum_{j=1}^{N}\frac{\hat{p}_j^2}{2m} + \hbar\frac{g}{2}\sum_{j=1}^{N}(\hat{a}^\dagger\hat{\sigma}_j^- + \hat{\sigma}_j^+\hat{a})\cos(k\hat{x}_j),$$

(1)

where $\Delta = \omega_c - \omega_a$. We have introduced the bosonic annihilation and creation operators, $\hat{a}$ and $\hat{a}^\dagger$, for cavity photons. The jth atom is represented by Pauli pseudospin operators, $\hat{\sigma}_j^z$ and $\hat{\sigma}_j^- = (\hat{\sigma}_j^+)^\dagger$, and position and momentum $\hat{x}_j$ and $\hat{p}_j$, respectively.

In the presence of dissipation, the evolution of the system is described by the Born-Markov quantum master equation for the density matrix $\hat{\rho}$ for the cavity and atoms,

$$\frac{d}{dt}\hat{\rho} = \frac{1}{i\hbar}[\hat{H},\rho] + \kappa\mathcal{L}[\hat{a}]\rho + w\sum_{j=1}^{N}\int_{-1}^{1}du N(u)\mathcal{L}[\hat{\sigma}_j^+ e^{iuk'\hat{x}_j}]\rho,$$

(2)

where $\mathcal{L}[\hat{O}]\hat{\rho} = (2\hat{O}\hat{\rho}\hat{O}^\dagger - \hat{O}^\dagger\hat{O}\hat{\rho} - \hat{\rho}\hat{O}^\dagger\hat{O})/2$ is the Linbladian superoperator describing the incoherent processes. The term proportional to κ describes the cavity decay. The repumping is the term proportional to w and is modeled by spontaneous absorption with recoil [33]. The recoil is parametrized by the normalized emission pattern $N(u)$ and wave vector k'. We neglect free-space spontaneous emission, since the natural linewidth γ is assumed to be extremely small for atoms with an ultraweak-dipole transition.

In the regime of interest, the cavity linewidth is much larger than other system frequencies, and the cavity field can be adiabatically eliminated, resulting in phase locking of the cavity field to the collective atomic dipole [26,29,30]. In order to correctly encapsulate the cavity cooling mechanism, the adiabatic elimination of the cavity field must be expanded beyond leading order. This includes retardation effects between the cavity field and atomic variables. As shown in the Supplemental Material [34], in the large κ limit [35],

$$\hat{a}(t) \approx \frac{-i\frac{g}{2}\hat{J}^-}{\kappa/2 + i\Delta} + \frac{\frac{d}{dt}(i\frac{g}{2}\hat{J}^-)}{(\kappa/2 + i\Delta)^2} - \frac{2i\sqrt{\Gamma_C}}{g}\hat{\xi}(t) + \mathcal{O}[\kappa^{-3}],$$

(3)

where $\hat{J}^- = \sum_{j=1}^{N}\hat{\sigma}_j^-\cos(k\hat{x}_j)$ is the collective dipole operator, $\Gamma_C = g^2\kappa/4(\kappa^2/4 + \Delta^2)$ is the spontaneous emission rate through the cavity, and $\hat{\xi}(t)$ is the quantum noise originating from the vacuum field entering through the cavity output.

The dipole force on the jth atom is given by the gradient of the potential energy, which takes the form

$$F_j = \frac{d}{dt}\hat{p}_j = -\nabla_j\hat{H} = \frac{1}{2}\hbar kg\sin(k\hat{x}_j)(\hat{\sigma}_j^+\hat{a} + \hat{a}^\dagger\hat{\sigma}_j^-).$$

(4)

We maximize the single-atom dissipative force by working at the detuning $\Delta = \kappa/2$ [34], and in that case by substituting Eq. (3) into Eq. (4), we find

$$\frac{d}{dt}\hat{p}_j \approx -\frac{1}{2}\hbar k\Gamma_C\sin(k\hat{x}_j)((1+i)\hat{\sigma}_j^+\hat{J}^- + (1-i)\hat{J}^+\hat{\sigma}_j^-)$$
$$-\frac{1}{2}\eta\Gamma_C\sin(k\hat{x}_j)\sum_{l=1}^{N}(\hat{\sigma}_j^+\hat{\sigma}_l^- + \hat{\sigma}_l^+\hat{\sigma}_j^-)\frac{1}{2}[\sin(k\hat{x}_l),\hat{p}_l]_+$$
$$+\hat{\mathcal{N}}_j.$$

(5)

Here the anticommutator is $[\hat{A},\hat{B}]_+ = \hat{A}\hat{B} + \hat{B}\hat{A}$. We have defined $\eta = 4\omega_r/\kappa$, which characterizes the likelihood that a photon emission into the cavity mode will be in the same direction as the motion, in terms of the recoil frequency $\omega_r = \hbar k^2/2m$. The three terms on the right-hand side of Eq. (5) can be interpreted as the conservative force, the friction, and the noise-induced momentum fluctuations, respectively.

For temperatures above the recoil temperature, the motion is well described by a semiclassical treatment. A systematic semiclassical approximation, to make the mapping $\langle\hat{x}_j\rangle \rightarrow x_j$ and $\langle\hat{p}_j\rangle \rightarrow p_j$, where x_j and p_j are classical variables, is based on the symmetric ordering of operator expectation values. In order to accurately incorporate the effects of quantum noise, we match the equations of motion for the second-order moments of momenta between the quantum and semiclassical theories so that

we obtain the correct momentum diffusion [34]. This procedure yields Ito stochastic equations,

$$\frac{d}{dt}p_j \approx \hbar k \Gamma_C \sin(kx_j)(\text{Im}[\langle \hat{\sigma}_j^+ \hat{J}^- \rangle] - \text{Re}[\langle \hat{\sigma}_j^+ \hat{J}^- \rangle])$$

$$- \eta \Gamma_C \sin(kx_j) \sum_{l=1}^{N} \text{Re}[\langle \hat{\sigma}_j^+ \hat{\sigma}_l^- \rangle] \sin(kx_l)p_l + \xi_j^p, \tag{6}$$

where ξ_j^p is the classical noise and $\langle \xi_j^p(t)\xi_l^p(t') \rangle = D^{jl}\delta(t-t')$ with diffusion matrix

$$D^{jl} = \hbar^2 k^2 \Gamma_C \sin(kx_j) \sin(kx_l)\text{Re}[\langle \hat{\sigma}_l^+ \hat{\sigma}_j^- \rangle]$$

$$+ \hbar^2 k'^2 w \bar{u^2} \langle \hat{\sigma}_j^- \hat{\sigma}_l^+ \rangle \delta_{jl}, \tag{7}$$

involving the geometrical average $\bar{u^2} \equiv \int_{-1}^{1} u^2 N(u)du$ and Kronecker delta δ_{jl}. The momentum evolution is paired with the usual equation for x_j,

$$\frac{d}{dt}x_j = \frac{p_j}{m}. \tag{8}$$

We first consider the case in which the effect of recoil associated with the repumping is neglected; i.e., we set $k' = 0$. This determines the ultimate temperature limit imposed by the vacuum noise due to the cavity output. For the one-atom case, we can then find the friction (α) and diffusion (D) coefficient from Eq. (6) and Eq. (7). The steady-state temperature T for the single atom (labeled by 1) is

$$k_B T = \frac{\langle p_1^2 \rangle}{m} = \frac{D}{2m\alpha} = \frac{\hbar \kappa}{4}, \tag{9}$$

since

$$D = \hbar^2 k^2 \Gamma_C \sin^2(kx_1)\langle \hat{\sigma}_1^+ \hat{\sigma}_1^- \rangle,$$

$$\alpha = \eta \Gamma_C \sin^2(kx_1)\langle \hat{\sigma}_1^+ \hat{\sigma}_1^- \rangle. \tag{10}$$

Note that this is precisely the same temperature limit previously found in the cavity-assisted cooling case where the system is operating in the strong coupling cavity-QED region. Here the rate of the decay into the cavity mode is proportional to $\Gamma_C \langle \hat{\sigma}_1^+ \hat{\sigma}_1^- \rangle$, which is applicable to the weak coupling regime of cavity QED [31]. In Fig. 2(a), we show a numerical simulation of the cooling trajectory of a single atom as a function of time. As expected, the final temperature $k_B T$ asymptotes to $\hbar \kappa / 4$ and the cooling rate is well approximated by $R_S = \eta \Gamma_C \langle \hat{\sigma}_1^+ \hat{\sigma}_1^- \rangle$.

The cooling in the many-atom case exhibits a distinctly different character. A feature of this model is the pseudospin-to-motion coupling of the atoms. In order to close the evolution equations of the atomic motion as described by Eq. (6) and Eq. (8), it is necessary to solve the pseudospin dynamics. For this purpose, we derive in the Supplemental Material [34] the quantum master equation for the pseudospins,
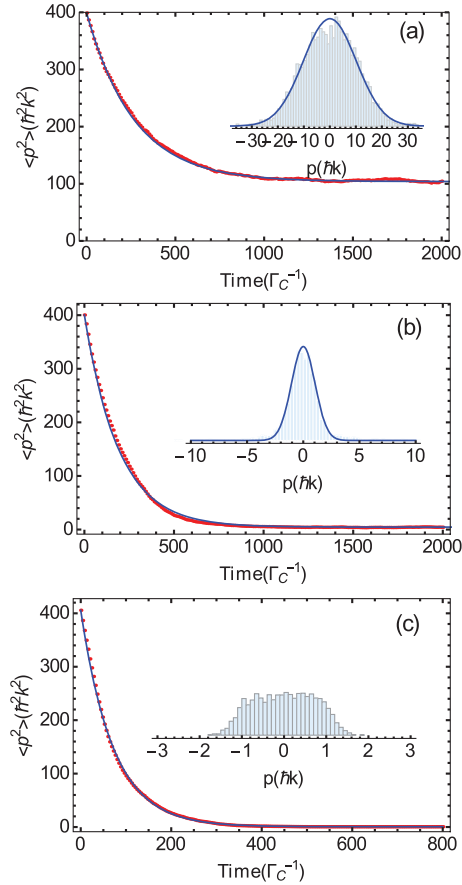

FIG. 2. Time evolution of the average momentum square (red dots) evaluated from 4000 trajectories simulated by integrating Eqs. (6) and (8) for 1 (a), 20 (b), and 60 atoms (c). The blue solid line is a fit to an exponential decay. The parameters are $\Delta = \kappa/2 = 100$, $\Gamma_C = 0.1$, and $\omega_r = 0.25$. The repumping rates are chosen such that the average atomic population inversion in all cases is the same [$w = 0.15$ (a), 0.28 (b), 1.3 (c)]. Insets show the momentum statistics. The blue solid line is a fit to a Gaussian distribution.

$$\frac{d}{dt}\hat{\rho} = \frac{1}{i\hbar}[\hat{H}_{\text{eff}}, \hat{\rho}] + \Gamma_C \mathcal{L}[\hat{J}^-]\hat{\rho}$$

$$+ w \sum_{j=1}^{N} \int_{-1}^{1} du N(u)\mathcal{L}[\hat{\sigma}_j^+ e^{iuk'\hat{x}_j}]\rho, \tag{11}$$

where the effective Hamiltonian $\hat{H}_{\text{eff}} = -\hbar \Gamma_C \hat{J}^+ \hat{J}^- /2$ describes the coherent coupling between atoms, and the collective decay [term proportional to Γ_C in Eq. (11)] leads to dissipative coupling. It is the dissipative coupling that gives rise to dipole synchronization and steady-state superradiance [25–30]. The full pseudospin Hilbert space dimension scales exponentially with the atom number. To solve Eq. (11), we employ a cumulant approximation that is applicable to many atoms [26,29,30]. All nonzero observables are expanded in terms of $\langle \hat{\sigma}_j^+ \hat{\sigma}_j^- \rangle$ and $\langle \hat{\sigma}_j^+ \hat{\sigma}_l^- \rangle$ ($j \neq l$), describing the population inversion and spin-spin
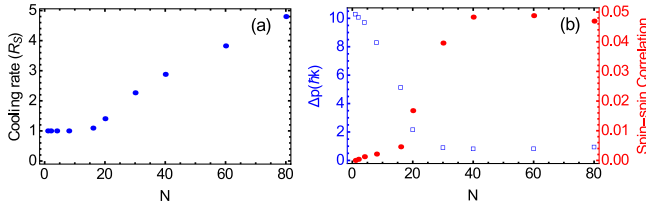
FIG. 3. (a) Cooling rate (in units of the single atom cooling rate R_S) as a function of atom number. (b) Final momentum width ($\Delta p = \sqrt{\langle p^2 \rangle}$, blue squares) and spin-spin correlation (red dots) as a function of atom number. The parameters are the same as those in Fig. 2.

correlations, respectively. Their equations of motion are derived in the Supplemental Material [34].

Simulations of the cooling dynamics for many atoms are shown in Figs. 2(b) and 2(c). Remarkably, we find the collective atomic effects lead to a more rapid cooling rate, and, simultaneously, to a lower final temperature. Figure 3 shows the cooling rate (a) and the final momentum width (b) as a function of the atom number. We note that the cooling rate exhibits two kinds of behavior, hinting towards the existence of an N-dependent threshold; see Fig. 3(a). For $N \lesssim 20$, the cooling rate is independent of N, while for $N \gtrsim 20$, it increases monotonically. Correspondingly, in this regime, the momentum width reaches a minimum independent of N; see Fig. 3(b). When the final temperature gets closer to the recoil temperature, the momentum distribution is no longer Gaussian, rendering the notion of temperature invalid. The semiclassical treatment predicts a uniform distribution in the momentum interval $[-\hbar k, \hbar k]$ corresponding to the recoil limit, as shown in the inset of Fig. 2(c). We note that sub-Doppler temperatures for a similar setup have been reported in Refs. [36–38], where spontaneous decay was assumed to be the fastest incoherent process. Differing from that regime, the recoil limit is here reached thanks to the small spontaneous decay rate. When the temperature approaches the recoil temperature, however, the validity of the semiclassical treatment of atomic motion is questionable and a full quantum model is necessary in order to determine the asymptotic energy. These results demonstrate that not only is the cooling more efficient due to the rapid rate of superradiant light emission, but also the final temperature is determined by the relaxation rate Γ_C of the atomic dipole, and not by the cavity linewidth.

The principal new feature is that spin-spin correlations between atoms develop due to the cavity-mediated coupling. In order to measure the extent of this effect, we introduce $\langle \hat{\sigma}^+ \hat{\sigma}^- \rangle_E$ defined as averaged spin-spin correlations,

$$\langle \hat{\sigma}^+ \hat{\sigma}^- \rangle_E = \left(\langle \hat{J}^+ \hat{J}^- \rangle - \sum_{j=1}^{N} \langle \hat{\sigma}_j^+ \hat{\sigma}_j^- \rangle \cos^2(kx_j) \right) / [N(N-1)].$$

(12)

Figure 3(b) shows $\langle \hat{\sigma}^+ \hat{\sigma}^- \rangle_E$ as a function of the atom number. The equilibrium temperature decreases as the collective spin-spin correlation emerges. This is reminiscent of the linewidth of the superradiant laser, where the synchronization of spins leads to a significant reduction of the linewidth to the order of Γ_C [25,30]. The establishment of spin-spin correlations is a competition between dephasing due to both cavity output noise and repumping, and the dissipative coupling between atoms which tends to synchronize the dipoles [30]. Since the coupling strength scales with N, a sufficient atom number is required to establish strong spin-spin correlations [30].

Further characterizing the ultimate temperature limits, Fig. 4(a) shows the final momentum width as a function of Γ_C. We see that as Γ_C is decreased, the final temperature reduces in proportion to Γ_C until it hits the recoil limit. This effect is consistent with a significantly increased friction coefficient providing a reduction of the order of the final temperature from the one to many atom case from κ to Γ_C.

So far our discussion has neglected the recoil associated with repumping. We have done that because its effect on the final temperature will depend crucially on specifics of its implementation, including factors such as the polarizations and directions of repump lasers, the atomic system, and the transitions used. However, in the specific repumping model shown in Fig. 1, the magnitude of k' controls the recoil effect of the repumping on the momentum diffusion. Figure 4(b) shows the final momentum width as a function of repumping for $k' = 0$ and $k' = k$. Again, in the region of small and large repumping, where spin-spin correlations are very small, the final temperature is high. When the recoil due to repumping is included, the final temperature becomes higher and is eventually determined by $w\bar{u}^2$. However, for weak repumping, with w not significantly larger then Γ_C it is still possible to achieve temperatures not much higher than that predicted when pump recoil was neglected. This is especially promising for the implementation of supercooling in realistic experimental systems. Note that $k = k'$ is more or less a worst case scenario, since by using a dipole allowed transition for the relaxation from the auxiliary state to the excited state, one could, in
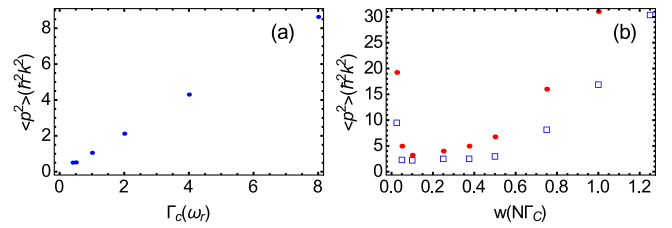

FIG. 4. (a) Final momentum width as a function of Γ_C for 40 atoms. The parameters are $\Delta = \kappa/2 = 200$, $w = N\Gamma_C/4$, and $\omega_r = 0.25$. (b) Final momentum width as a function of repumping strength for 40 atoms without ($k' = 0$, blue squares) and with recoil associated with repumping ($k' = k$, red dots). The parameters are $\Delta = \kappa/2 = 200$, $\Gamma_C = 0.5$, and $\omega_r = 0.25$.

principle, use a much reduced frequency with correspondingly small recoil.

In conclusion, we have proposed supercooling of the atomic motion along the axis of an optical cavity. The superradiant emission was observed to lead to an enhanced cooling rate and extremely low final temperature. The ultimate temperatures were constrained by the relaxation of the atomic dipole, and may be orders of magnitude lower than for single atom cooling where temperatures are limited by the cavity linewidth. From a broader viewpoint, we have demonstrated an example of many-body laser cooling in which all motional degrees of freedom of a collective system are simultaneously cooled, and in which macroscopic spin-spin correlations are essential and must develop for the cooling mechanism to work.

[1] C. E. Wieman, D. E. Pritchard, and D. J. Wineland, Rev. Mod. Phys. **71**, S253 (1999).

[2] I. Bloch, J. Dalibard, and W. Zwerger, Rev. Mod. Phys. **80**, 885 (2008).

[3] A. D. Ludlow, M. M. Boyd, J. Ye, E. Peik, and P. O. Schmidt, Rev. Mod. Phys. **87**, 637 (2015).

[4] I. A. Walmsley, Science **348**, 525 (2015).

[5] D. J. Wineland, Rev. Mod. Phys. **85**, 1103 (2013).

[6] T. W. Hänsch and A. L. Schawlow, Opt. Commun. **13**, 68 (1975).

[7] D. J. Wineland and W. M. Itano, Phys. Rev. A **20**, 1521 (1979).

[8] P. Domokos and H. Ritsch, J. Opt. Soc. Am. B **20**, 1098 (2003).

[9] H. Ritsch, P. Domokos, F. Brennecke, and T. Esslinger, Rev. Mod. Phys. **85**, 553 (2013).

[10] P. Horak, G. Hechenblaikner, K. M. Gheri, H. Stecher, and H. Ritsch, Phys. Rev. Lett. **79**, 4974 (1997).

[11] V. Vuletić and S. Chu, Phys. Rev. Lett. **84**, 3787 (2000).

[12] J. McKeever, J. R. Buck, A. D. Boozer, A. Kuzmich, H.-C. Nägerl, D. M. Stamper-Kurn, and H. J. Kimble, Phys. Rev. Lett. **90**, 133602 (2003).

[13] P. Maunz, T. Puppe, I. Schuster, N. Syassen, P. W. H. Pinkse, and G. Rempe, Nature (London) **428**, 50 (2004).

[14] D. R. Leibrandt, J. Labaziewicz, V. Vuletić, and I. L. Chuang, Phys. Rev. Lett. **103**, 103001 (2009).

[15] M. H. Schleier-Smith, I. D. Leroux, H. Zhang, M. A. Van Camp, and V. Vuletić, Phys. Rev. Lett. **107**, 143005 (2011).

[16] M. Wolke, J. Klinner, H. Kessler, and A. Hemmerich, Science **337**, 75 (2012).

[17] G. Morigi, P. W. H. Pinkse, M. Kowalewski, and R. deVivie-Riedle, Phys. Rev. Lett. **99**, 073001 (2007).

[18] B. L. Lev, A. Vukics, E. R. Hudson, B. C. Sawyer, P. Domokos, H. Ritsch, and J. Ye, Phys. Rev. A **77**, 023402 (2008).

[19] N. Kiesel, F. Blaser, U. Delic, D. Grass, R. Kaltenbaek, and M. Aspelmeyer, Proc. Natl. Acad. Sci. U.S.A. **110**, 14180 (2013).

[20] J. Millen, P. Z. G. Fonseca, T. Mavrogordatos, T. S. Monteiro, and P. F. Barker, Phys. Rev. Lett. **114**, 123602 (2015).

[21] P. Domokos and H. Ritsch, Phys. Rev. Lett. **89**, 253003 (2002).

[22] H. W. Chan, A. T. Black, and V. Vuletić, Phys. Rev. Lett. **90**, 063003 (2003).

[23] K. J. Arnold, M. P. Baden, and M. D. Barrett, Phys. Rev. Lett. **109**, 153002 (2012).

[24] S. Schütz and G. Morigi, Phys. Rev. Lett. **113**, 203002 (2014).

[25] D. Meiser, J. Ye, D. R. Carlson, and M. J. Holland, Phys. Rev. Lett. **102**, 163601 (2009).

[26] D. Meiser and M. J. Holland, Phys. Rev. A **81**, 033847 (2010); **81**, 063827 (2010).

[27] J. G. Bohnet, Z. Chen, J. M. Weiner, D. Meiser, M. J. Holland, and J. K. Thompson, Nature (London) **484**, 78 (2012).

[28] J. G. Bohnet, Z. Chen, J. M. Weiner, K. C. Cox, and J. K. Thompson, Phys. Rev. Lett. **109**, 253602 (2012).

[29] Minghui Xu, D. A. Tieri, E. C. Fine, J. K. Thompson, and M. J. Holland, Phys. Rev. Lett. **113**, 154101 (2014).

[30] Minghui Xu and M. J. Holland, Phys. Rev. Lett. **114**, 103601 (2015).

[31] P. Meystre and M. Sargent III, *Elements of Quantum Optics* (Springer, New York, 1998).

[32] The finite spatial mode of the cavity causes a spread in g. This leads to a reduced effective atom number, which has no significant impact on the cooling mechanisms discussed in this Letter.

[33] H. Haken, *Laser Theory* (Springer, Berlin, 1984).

[34] See Supplemental Material at http://link.aps.org/supplemental/10.1103/PhysRevLett.116.153002, which includes Refs. [26,29], for the derivation of the equations for the adiabatic elimination of the cavity mode, for the external motion of atoms, and for the internal dynamics of atoms.

[35] This requires $\kappa \gg \sqrt{N\bar{n}}g$, w, and $k\sqrt{\langle p^2 \rangle}/m$, where $\bar{n}$ is the mean photon number in the cavity.

[36] T. Salzburger and H. Ritsch, Phys. Rev. Lett. **93**, 063002 (2004).

[37] T. Salzburger, P. Domokos, and H. Ritsch, Phys. Rev. A **72**, 033805 (2005).

[38] T. Salzburger and H. Ritsch, Phys. Rev. A **74**, 033806 (2006).